

## Atomistic Picture of Charge Density Wave Formation at Surfaces

Simone Wall,<sup>1,\*†</sup> Boris Krenzer,<sup>1</sup> Stefan Wippermann,<sup>2,‡</sup> Simone Sanna,<sup>2</sup> Friedrich Klasing,<sup>1</sup> Anja Hanisch-Blicharski,<sup>1</sup> Martin Kammler,<sup>1,§</sup> Wolf Gero Schmidt,<sup>2</sup> and Michael Horn-von Hoegen<sup>1</sup>

<sup>1</sup>*Department of Physics and Center for Nanointegration Duisburg-Essen (CENIDE), University Duisburg-Essen, D-47057 Duisburg, Germany*

<sup>2</sup>*Chair of Theoretical Physics, Paderborn University, D-33095 Paderborn, Germany*

(Received 25 June 2012; published 2 November 2012)

We used ultrafast electron diffraction and density-functional theory calculations to gain insight into the charge density wave (CDW) formation on In/Si(111). Weak excitation by a femtosecond-laser pulse results in the melting of the CDW. The immediate freezing is hindered by a barrier for the motion of atoms during the phase transition: The melted CDW constitutes a long-lived, supercooled phase and is strong evidence for a first-order transition. The freezing into the CDW is triggered by preexisting adsorbates. Starting at these condensation nuclei, the CDW expands one dimensionally on the In/Si(111) surface, with a constant velocity of more than 80 m/s.

DOI: [10.1103/PhysRevLett.109.186101](https://doi.org/10.1103/PhysRevLett.109.186101)

PACS numbers: 68.35.Rh, 61.05.jh, 68.43.Bc, 71.45.Lr

Phase transitions in condensed matter are accompanied by a change in the electronic and geometric structure. The transition requires the collective motion of atoms on a complicated reaction path from one minimum of the multidimensional potential energy landscape to another. The presence of a barrier strongly affects the dynamics of such processes and defines a phase transition as a first-order transition. If the barrier is too high, the system remains in a metastable state for a long time without being able to reach the ground state. However, by the insertion of seeds the collapse of the system into the ground state may be triggered.

In strictly one-dimensional (1D) systems with short-range interactions there can be no phase transitions (see, e.g., Ref. [1]). This may change for real, quasi-1D systems due to the coupling to the environment. Highly anisotropic surface reconstructions are frequently used to study phenomena of 1D physics like non-Fermi liquidity [2] or the formation of Peierls condensates [3]. The indium-induced  $(8 \times 2)/(4 \times 1)$  reconstruction of the Si(111) surface [see Figs. 1(a) and 1(b)] is one of the most intensively investigated model systems in this context. It features a metal-insulator transition, the atomic mechanism of which has been elusive for a long time; see, e.g., Refs. [3,4]. At room temperature, the  $(4 \times 1)$  phase is a quasi-1D conductor. Upon cooling, it transforms into a nonconducting  $(8 \times 2)$  low-temperature phase by a Peierls-like distortion [5,6] corresponding to the formation of a charge density wave (CDW) [3,7–14]. The phase transition is facilitated by the opening of a fundamental band gap of the order of 100 meV which lowers the total energy of the electron system [7].

In this Letter, we use ultrafast electron diffraction and density functional calculations to gain insight into the CDW formation on In/Si(111). Initially, a transition from the low-temperature  $(8 \times 2)$  ground state into the excited  $(4 \times 1)$  state was triggered electronically by a

femtosecond-laser pulse resulting almost instantaneously in a melting of the CDW, as already reported for optical excitations of CDWs in bulk systems [15–17]. The immediate *freezing* back into the CDW is hindered by an energy barrier; thus the melted CDW remains in a long-lived, supercooled excited phase. The freezing back into the CDW is ultimately triggered by preexisting adsorbates: Starting at the condensation nuclei, the CDW expands one-dimensionally on the In/Si(111) surface, with a constant velocity.

The experiments were performed under ultrahigh vacuum conditions at a base pressure of  $2 \times 10^{-10}$  mbar. The samples, each of which had a width of 2 mm, were cut from commercial Si wafers, and mounted on a liquid helium cryostat, allowing for sample cooling with liquid helium to a base temperature of 20 K. Clean Si surfaces were prepared by short flash-anneal cycles up to 1500 K. The  $(8 \times 2)$  In/Si(111) reconstruction was prepared *in situ* by indium deposition on a clean silicon sample at a substrate temperature of 700 K. The integrity of the reconstruction during deposition, prior to deposition, and after each experiment was confirmed by low energy electron diffraction and reflection high energy electron diffraction (RHEED).

The melting and freezing of the CDW was observed by ultrafast time-resolved RHEED applying a pump-probe scheme in which the laser pulses excite the sample and variable delayed electron pulses probe its subsequent evolution [18]. Laser pulses of approximately 50 fs duration at 800 nm (1.55 eV) from a 5 kHz chirped pulse amplified titanium sapphire laser were used for the excitation of the  $(8 \times 2)$  In/Si(111) CDW phase at a fluence of  $2.1 \text{ mJ/cm}^2$ . The excited sample area ( $3 \times 2 \text{ mm}^2$ ) was larger than the area probed by the electron beam ( $0.4 \times 2 \text{ mm}^2$ ). Ultrashort electron pulses were generated through photoemission from a thin Au-cathode backilluminated by a femtosecond-laser pulse [19]. Diffraction

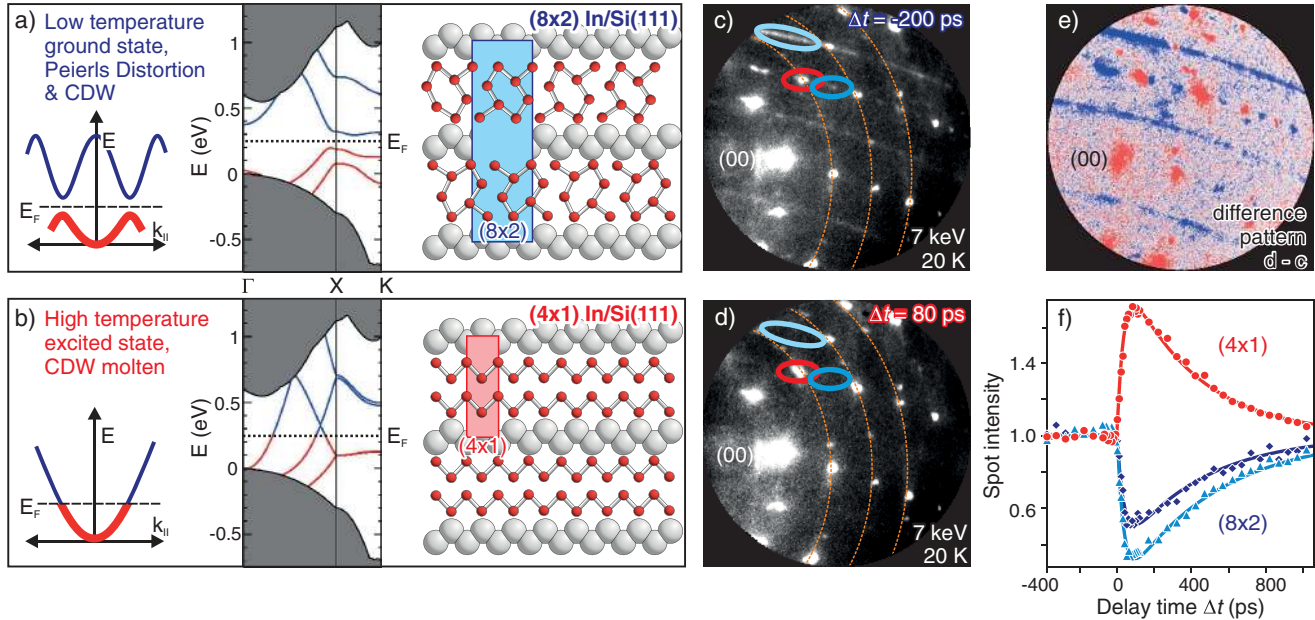


FIG. 1 (color). (a) The  $(8 \times 2)$  ground state exhibits a Peierls distortion with the formation of a CDW. (b) The high temperature phase is metallic, and the Peierls distortion is lifted. Atomic structure of the In-induced surface reconstruction on Si(111) [24] and calculated band structures of the hexagon model (a) and zigzag chain (b) of the In-Si(111) surface calculated by using density functional theory within a  $(4 \times 2)$  surface unit cell. RHEED patterns recorded at 20 K: (c) is taken prior to excitation depicting the  $(8 \times 2)$  ground state, and (d) is taken after laser excitation at a delay of 80 ps. The  $8 \times$  spots and twofold streaks have disappeared. (e) Difference image of the two RHEED patterns. Blue corresponds to an intensity decrease, and red to an increase: the  $8 \times$  spots and twofold streaks disappear while the  $(4 \times 1)$  spots become stronger. (f) Transient intensity evolution of the RHEED spots upon excitation at 20 K and a laser fluence of  $2.1 \text{ mJ/cm}^2$ . Solid lines describe an exponential fit.

patterns were taken as a function of the time delay between the excitation of the sample by an initial femtosecond-laser pulse (pump) and the electron pulse (probe). Electrons with an energy of 7 keV were diffracted at a grazing angle of incidence of  $\sim 5^\circ$  at the surface. The diffraction patterns were intensified by using a microchannel plate detector and recorded by a cooled CCD camera.

The change in the RHEED pattern upon excitation is evident from Fig. 1. The pattern in Fig. 1(c) was taken prior to the temporal overlap and shows the  $(8 \times 2)$  ground state. The twofold streaks and  $8 \times$  spots are clearly visible. The pattern in Fig. 1(d) was taken after excitation at a delay time of 80 ps and depicts the excited state. The twofold streaks and the  $8 \times$  spots have vanished, and only the  $(4 \times 1)$  spots are still visible; this means that the phase transition took place. This transition is even more obvious from Fig. 1(e) where a RHEED pattern without pump pulse is subtracted from a RHEED pattern with pump pulse. Blue colors indicate intensity loss, and red colors indicate intensity gain. All the  $8 \times$  spots and all the twofold streaks disappeared, while the  $(4 \times 1)$  spot intensity increased. The intensity of the  $(4 \times 1)$  spots (red),  $8 \times$  spots (blue), and twofold streaks (light blue) are plotted versus the delay time in Fig. 1(f). Within our temporal resolution, the intensity rise of the  $(4 \times 1)$  spots and the decay of the  $8 \times$  spots and the twofold streaks occurred simultaneously. In addition, the time constants for the deexcitation (red)

and the recovery of the ground state (light and dark blue) are almost identical with  $\tau = 440 \text{ ps}$ .

The clearly visible intensity increase of the  $(4 \times 1)$  spots cannot be explained by surface heating. Because of the Debye-Waller effect an increase in temperatures results in an intensity decrease [20]. It is therefore imperative to conclude that a structural transition of the geometric position of the atoms in the surface unit cell took place.

To further rule out a thermal excitation of the phase transition, we determined the maximum rise of the surface temperature caused by the laser pulse from the Debye-Waller effect [21,22] using the  $(4 \times 1)$  reconstruction. Assuming that the absorption coefficient for 1.55 eV photons is the same for both the  $(4 \times 1)$  and the  $(8 \times 2)$  reconstruction, a maximum temperature change  $\Delta T < 10 \text{ K}$  is obtained. This almost negligible rise in temperature excludes a thermal excitation of the phase transition: The sample cannot be heated from a base temperature of 20 K beyond the phase transition temperature that has been measured [7,8,10,12,14] and calculated [23] to lie between 95 and 130 K. It is concluded that the transition to the  $(4 \times 1)$  phase, i.e., the melting of the CDW, is solely electronically driven.

Upon excitation with the femtosecond-laser pulse, electron hole pairs were generated. Thermalization of the electron system results in the occupation of conduction band states close to the fundamental gap. Thus, the driving

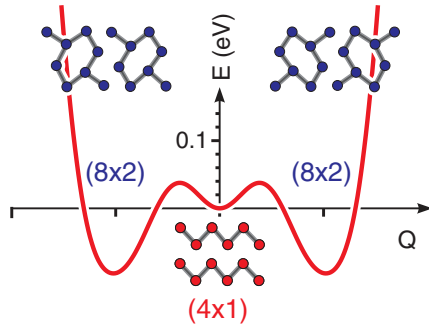


FIG. 2 (color). Energetics of the phase transition. Calculated total energy per  $(8 \times 2)$  surface unit cell in dependence of the reaction coordinate  $Q$  describing the  $(4 \times 1) - (8 \times 2)$  phase transition. The transition from the metastable  $(4 \times 1)$  phase into the  $(8 \times 2)$  ground state is hampered by an energy barrier of 40 meV.

force for the Peierls-like distortion is lifted. Consequently, the semiconducting  $(8 \times 2)$  reconstruction of the CDW ground state changes into the metallic  $(4 \times 1)$  phase. The observed time constant of  $\tau = 440$  ps for the recovery of the  $(8 \times 2)$  ground state, however, is surprisingly long compared to lifetimes of electronic excitations at surfaces, which are typically well below 10 ps. The mechanism of the Peierls instability-driven  $(8 \times 2) - (4 \times 1)$  phase transition has been controversially discussed since its discovery. As recently reviewed in Refs. [3,4,24], some authors argue in favor of a first-order transition, while others find indications for a second-order process. Both order-disorder and displacive mechanisms are discussed for the phase change. The present demonstration of a long-lived, metastable  $(4 \times 1)$  phase far away from thermal equilibrium rules out the order-disorder scenario and is strong evidence for a first-order transition.

In order to gain deeper insight into the energetics of the phase transition, we performed density-functional calculations using the VASP package [25] with computational details corresponding to the ones in Ref. [23]. The surface energy of the indium-reconstructed Si(111) is plotted in Fig. 2 along the generalized reaction coordinate  $Q$  obtained by superimposing the soft shear and rotary phonon eigenvectors that transform between the  $(4 \times 1)$  and the  $(8 \times 2)$  phase [24]. We found the transition from the  $(4 \times 1)$  phase to the  $(8 \times 2)$  structure to be hampered by an energy barrier of about 40 meV. Thus, a long-lived excited surface phase may indeed form: The system is then trapped in a metastable  $(4 \times 1)$  excited state. In analogy to a supercooled liquid, one might even expect the freezing, i.e., the transition back to the  $(8 \times 2)$  ground state, to be facilitated by condensation nuclei, possibly in form of adsorbates.

To verify this assumption experimentally, we monitored the phase transition dynamics upon controlled adsorption of molecules from the residual gas. The transient intensity evolution of the  $(8 \times 2)$  (black to green dots) and  $(4 \times 1)$  spots (red to yellow dots) is plotted in Fig. 3(a) for various

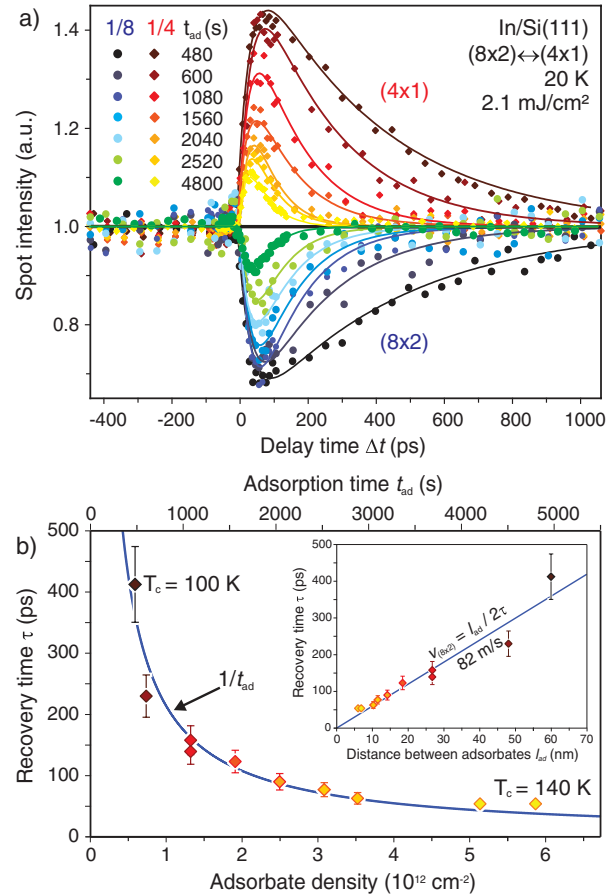


FIG. 3 (color). Recovery of the  $(8 \times 2)$  ground state. (a) The recovery of the  $(8 \times 2)$  ground state strongly depends on adsorption from the residual gas. With increasing adsorbate density the recovery time constant  $\tau$  changes from  $\tau = 415$  ps for the first experiment after  $t_{\text{ad}} = 480$  s (dark red data points) to  $\tau = 54$  ps after  $t_{\text{ad}} = 4800$  s (light yellow data points). (b) Time constant  $\tau$  for the recovery of the  $(8 \times 2)$  reconstruction as a function of adsorbate density. The solid line describes a  $1/t_{\text{ad}}$  behavior. From the slope in the inset we derive a velocity of the propagating phase front of  $v_{(8 \times 2)} = 82$  m/s.

adsorption times  $t_{\text{ad}}$ . With increasing adsorbate coverage, we observed a strong decrease in the time constant, as depicted in Fig. 3(b). The shortest observed time constant was  $\tau = 54$  ps for an adsorption time of  $t_{\text{ad}} = 75$  min. The solid line shows a fit to a  $1/t_{\text{ad}}$  behavior. Obviously, the adsorption from the residual gas drastically shortens the recovery time of the  $(8 \times 2)$  ground state by almost a factor of 10.

Sticking to the analogy with a supercooled liquid, the insertion of seeds, i.e., condensation nuclei, initiates the freezing, which then propagates with constant velocity. Here, freezing means recovery of the  $(8 \times 2)$  ground state. Because of the highly anisotropic nature of the indium-induced Si surface reconstruction this phase front propagates only one-dimensionally along the direction of the indium chains. Therefore, the velocity of the phase

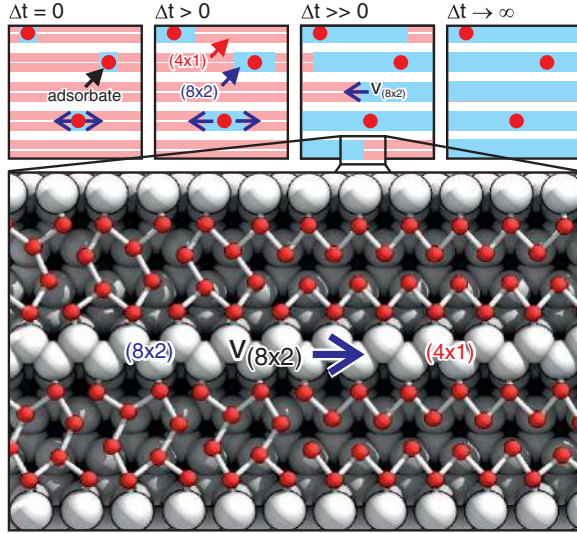


FIG. 4 (color). Propagation of the phase front of the  $(8 \times 2)$  ground state. Top: Adsorbates with a mean separation  $l_{ad}$  act as seeds (red dots).  $v_{(8 \times 2)}$  is the velocity of the propagating phase front. Bottom: A snapshot from the *ab initio* molecular dynamics simulations depicts the transition from the metastable  $(4 \times 1)$  phase to the  $(8 \times 2)$  ground state.

front  $v_{(8 \times 2)}$  within the one-dimensional In wire and the averaged distance  $l_{ad}$  between the condensation nuclei determine the time constant  $\tau$  for the complete recovery of the  $(8 \times 2)$  ground state:

$$\tau = l_{ad}/(2v_{(8 \times 2)}),$$

as sketched in Fig. 4. In addition, assuming a linear relation between adsorbate coverage  $\Theta_{ad}$  and the time  $t_{ad}$ , the distance between the adsorbates in one row obeys  $l_{ad} \propto t_{ad}^{-1}$ ; consequently, it holds  $\tau \propto t_{ad}^{-1}$ . This is indeed the experimental finding shown in Fig. 3(b). An estimate for the distance  $l_{ad}$  between adsorbates in one individual row can be obtained from the shift of critical temperature  $T_C$  as a function of the adsorbate density  $\Theta_{ad}$ . We observed  $\Delta T_C = +40$  K after adsorption for  $t_{ad} = 75$  min. According to Lee and Shibasaki [26,27], such a change in  $T_C$  is induced by an adsorbate density of  $\Theta_{ad} = 6 \times 10^{12}$  cm $^{-2}$  as determined by scanning tunneling microscopy [27]. The distance  $l_{ad}$  between the adsorbates, together with the measured time constant  $\tau$ , are sufficient to determine the lower limit of the phase front velocity  $v_{(8 \times 2)}$ . The present experimental data result in a value of  $v_{(8 \times 2)} = 82$  m/s. This value rests on the assumption that all adsorbates irrespective of species and adsorption site act as condensation nuclei and initiate a phase transition. However, due to the complexity of the  $(8 \times 2)$  surface reconstruction, not every adsorbate is likely to trigger a phase transition. In fact, it was found that some adsorbates stabilize the  $(4 \times 1)$  phase [26–28].

To obtain microscopic insight into the phase transition mechanism, we performed *ab initio* molecular dynamics

simulations [25] for the  $(4 \times 1)$  surface phase at 20 K using a  $(8 \times 12)$  slab with periodic boundary conditions. The simulations (a snapshot is shown in Fig. 4) confirm that the phase transition starts exclusively from condensation nuclei and propagates by changing the atomic structure of subsequent unit cells one after the other with an average velocity of  $v_{(8 \times 2)} = 850$  m/s. Comparing this value with the velocity of 82 m/s derived from the measured data, we conclude that not every adsorbate acts as a seed for the phase transition.

In summary, it is found that the CDW ground state of the In/Si(111) surface can be melted by femtosecond-laser excitation with negligible thermal heating of the surface. The periodicity doubling of the Peierls distortion is lifted, the band gap closes, and the surface becomes metallic. The instantaneous freezing of the CDW, i.e., the recovery of the Peierls-distorted ground state of the In/Si(111) system, is hampered by an energy barrier for the motion of atoms. A supercooled metastable surface phase far away from thermal equilibrium is created by laser excitation—a state of matter which otherwise is inaccessible. This supercooled surface phase can be observed at time scales much longer than picoseconds. The freezing of the CDW is ultimately triggered by heterogeneous nucleation of the ground state at adsorbates. It propagates from these preexisting seeds—comparable to a falling row of dominoes—roughly with the speed of sound.

We thank Jörg Schäfer, Klaus Sokolowski-Tinten, Manuel Ligges, Uwe Bovensiepen, and Dirk Wall for many fruitful discussions. Financial support from the Deutsche Forschungsgemeinschaft through SFB 616, “Energy Dissipation at Surfaces,” and FOR 1405, FOR 1700 as well as generous grants of supercomputer time provided by the HLRS Stuttgart and the Paderborn PC $^2$  are gratefully acknowledged.

\*simone.wall@uni-due.de

†Present address: Max-Planck-Institut für Kohlenforschung, Kaiser-Wilhelm-Platz 1, D-45470 Mülheim an der Ruhr, Germany.

‡Present address: Department of Chemistry, University of California, One Shields Avenue, Davis, CA 95616, USA.

§Present address: University of Applied Science, 93049 Regensburg, Germany.

- [1] E. Lieb and D. Mattis, *Mathematical Physics in One Dimension: Exactly Soluble Models of Interacting Particles* (Academic, New York, 1966).
- [2] C. Blumenstein, J. Schäfer, S. Mietke, S. Meyer, A. Dollinger, M. Lochner, X.Y. Cui, L. Patthey, R. Matzdorf, and R. Claessen, *Nat. Phys.* **7**, 776 (2011).
- [3] P. Snijders and H. Weitering, *Rev. Mod. Phys.* **82**, 307 (2010).
- [4] S. Hatta, Y. Ohtsubo, T. Aruga, S. Miyamoto, H. Okuyama, H. Tajiri, and O. Sakata, *Phys. Rev. B* **84**, 245321 (2011).

- [5] R. Peierls, *Ann. Phys. (Leipzig)* **396**, 121 (1930).
- [6] G. Gruener, *Rev. Mod. Phys.* **60**, 1129 (1988).
- [7] H. W. Yeom *et al.*, *Phys. Rev. Lett.* **82**, 4898 (1999).
- [8] Y. J. Sun, S. Agario, S. Souma, K. Sugawara, Y. Tago, T. Sato, and T. Takahashi, *Phys. Rev. B* **77**, 125115 (2008).
- [9] C. Gonzalez, F. Flores, and J. Ortega, *Phys. Rev. Lett.* **96**, 136101 (2006).
- [10] S. Park, H. Yeom, S. Min, D. Park, and I.-W. Lyo, *Phys. Rev. Lett.* **93**, 106402 (2004).
- [11] J. R. Ahn, J. H. Byun, H. Koh, E. Rotenberg, S. D. Kevan, and H. W. Yeom, *Phys. Rev. Lett.* **93**, 106401 (2004).
- [12] K. Fleischer, S. Chandola, N. Esser, W. Richter, and J. F. McGilp, *Phys. Rev. B* **67**, 235318 (2003).
- [13] S. V. Ryjkov, T. Nagao, V. G. Lifshits, and S. Hasegawa, *Surf. Sci.* **488**, 15 (2001).
- [14] C. Kumpf, O. Bunk, J. H. Zeysing, Y. Su, M. Nielsen, R. L. Johnson, R. Feidenhans'l, and K. Bechgaard, *Phys. Rev. Lett.* **85**, 4916 (2000).
- [15] F. Schmitt *et al.*, *Science* **321**, 1649 (2008).
- [16] M. Eichberger, H. Schafer, M. Krumova, M. Beyer, J. Demsar, H. Berger, G. Moriena, G. Sciaini, and R. J. D. Miller, *Nature (London)* **468**, 799 (2010).
- [17] J. C. Petersen *et al.*, *Phys. Rev. Lett.* **107**, 177402 (2011).
- [18] A. Janzen, B. Krenzer, P. Zhou, D. von der Linde, and M. Horn-von Hoegen, *Surf. Sci.* **600**, 4094 (2006).
- [19] A. Janzen, B. Krenzer, O. Heinz, P. Zhou, D. Thien, A. Hanisch, F.-J. Meyer zu Heringdorf, D. von der Linde, and M. Horn-von Hoegen, *Rev. Sci. Instrum.* **78**, 013906 (2007).
- [20] P. Debye, *Ann. Phys. (Leipzig)* **348**, 49 (1913).
- [21] B. Krenzer, A. Janzen, P. Zhou, D. von der Linde, and M. Horn-von Hoegen, *New J. Phys.* **8**, 190 (2006).
- [22] A. Hanisch, B. Krenzer, T. Pelka, S. Möllenbeck, and M. Horn-von Hoegen, *Phys. Rev. B* **77**, 125410 (2008).
- [23] S. Wippermann and W. G. Schmidt, *Phys. Rev. Lett.* **105**, 126102 (2010).
- [24] W. G. Schmidt, S. Wippermann, S. Sanna, M. Babilon, N. J. Vollmers, and U. Gerstmann, *Phys. Status Solidi B* **249**, 343 (2012).
- [25] G. Kresse and J. Furthmüller, *Comput. Mater. Sci.* **6**, 15 (1996).
- [26] G. Lee, S.-Y. Yu, H. Shim, W. Lee, and J.-Y. Koo, *Phys. Rev. B* **80**, 075411 (2009).
- [27] T. Shibusaki *et al.*, *Phys. Rev. B* **81**, 035314 (2010).
- [28] W. G. Schmidt, M. Babilon, C. Thierfelder, S. Sanna, and S. Wippermann, *Phys. Rev. B* **84**, 115416 (2011).